Structure *14*, 51–61, January 2006 DOI 10.1016/j.str.2005.09.015

A Second FMN Binding Site in Yeast NADPH-Cytochrome P450 Reductase Suggests a Mechanism of Electron Transfer by Diflavin Reductases

David C. Lamb,[1,4] Youngchang Kim,[3,4] Liudmila V. Yermalitskaya,[2] Valery N. Yermalitsky,[2] Galina I. Lepesheva,[2] Steven L. Kelly,[1] Michael R. Waterman,[2] and Larissa M. Podust[2,*]

[1]Wolfson Laboratory of P450 Biodiversity
Swansea Medical School University of Wales Swansea
Swansea, Wales, SA2 8PP
United Kingdom

[2]Department of Biochemistry
Vanderbilt University School of Medicine
Nashville, Tennessee 37232

[3]Argonne National Laboratory
Structural Biology Center
Argonne, Illinois 60439

Summary

NADPH-cytochrome P450 reductase transfers two reducing equivalents derived from a hydride ion of NADPH via FAD and FMN to the large family of microsomal cytochrome P450 monooxygenases in one-electron transfer steps. The mechanism of electron transfer by diflavin reductases remains elusive and controversial. Here, we determined the crystal structure of truncated yeast NADPH-cytochrome P450 reductase, which is functionally active toward its physiological substrate cytochrome P450, and discovered a second FMN binding site at the interface of the connecting and FMN binding domains. The two FMN binding sites have different accessibilities to the bulk solvent and different amino acid environments, suggesting stabilization of different electronic structures of the reduced flavin. Since only one FMN cofactor is required for function, a hypothetical mechanism of electron transfer is discussed that proposes shuttling of a single FMN between these two sites coupled with the transition between two semiquinone forms, neutral (blue) and anionic (red).

Introduction

The mechanism of electron transfer by diflavin reductases remains both elusive and controversial despite extensive studies including kinetic, spectroscopic, crystallographic, and site-directed mutagenesis techniques (Murataliev et al., 2004). Mechanisms proposed for mammalian (Backes, 1993) and other (Murataliev et al., 1997, 1999; Murataliev and Feyereisen, 1999; Sevrioukova et al., 1996a) NADPH-cytochrome P450 reductases (CPRs) disagree in (1) the number of electrons residing on flavins during the catalytic cycle, in (2) the requirement for a priming reaction by NADPH, and in (3) the active form of the FMN that serves as donor of electrons.

Within the cell, CPR is anchored to the endoplasmic reticulum through a single N-terminal amino acid segment and transfers electrons from NADPH to its major physiological acceptors, the ubiquitous family of microsomal cytochrome P450 monooxygenases (P450, CYP), as well as to squalene monooxygenase (Laden et al., 2000; Ono and Bloch, 1975), heme oxygenase (Schacter et al., 1972), fatty acid desaturase (Ilan et al., 1981), and cytochrome b5 (Enoch and Strittmatter, 1979). In vitro, CPR can donate electrons to the nonphysiological electron acceptor cytochrome c (Williams and Kamin, 1962) and to a variety of small-molecule dyes. Microsomal CPRs belong to a family of electron transporters that includes the *Bacillus megaterium* cytochrome P450 (P450BM3) reductase (Narhi and Fulco, 1986) and related homologs from *Bacillus subtilis* (Gustafsson et al., 2004) and *Fusarium oxysporum* (Kitazume et al., 2000), as well as nitric oxide synthases (Bredt et al., 1991), methionine synthase reductase (Leclerc et al., 1998), novel reductase 1 (Paine et al., 2000), and the α subunit of bacterial sulfite reductases (Ostrowski et al., 1989). The common feature of these reductases is the presence of two flavin prosthetic groups, FAD and FMN, which channel electrons from NADPH to metal ion centers. During a catalytic cycle, CPR transfers a hydride ion derived from NADPH to FAD, and the latter transfers electrons to FMN, from where they are delivered to acceptor proteins in two one-electron transfer steps. Diflavin reductases share significant sequence homology with two classes of flavoproteins, prokaryotic FMN-containing flavodoxin and FAD-containing ferredoxin-NADP$^+$ reductase (Porter and Kasper, 1985). This fact led to the hypothesis that diflavin reductases evolved as fusion proteins of the two bacterial monoflavin electron transport enzymes (Porter and Kasper, 1986). A connecting domain, unique for diflavin reductases, tethers the flavin binding domains close to each other to maximize electronic coupling (Coves et al., 1997; Sevrioukova et al., 1996b; Smith et al., 1994). Indeed, *Escherichia coli* flavoproteins, flavodoxin, and NADPH-flavodoxin reductase can serve as an electron transfer system for microsomal P450, although with rates an order of magnitude lower than CPR (Jenkins and Waterman, 1998).

When separately expressed, FAD/NADPH and FMN binding domains of human and rat reductases (Smith et al., 1994), P450BM3 (Sevrioukova et al., 1997), and the *E. coli* sulfite reductase (Coves et al., 1997) reconstitute very low (0%–6%) catalytic activities of P450 and nonphysiological partners. The low level of CPR activity obtained by combining the individual reductase domains may suggest that evolution leaned toward fused diflavin reductases, resulting in a conceptually new electron transport mechanism rather than in a simple sum of properties of the two individual monoflavin ancestors.

The only resolved CPR crystal structure to date that shows the interactions between all structural domains is that for N-terminal truncated rat CPR (rCPR) (Wang et al., 1997). However, a limitation of this structure comes from the fact that although truncated rCPR can reduce cytochrome c, it is totally inactive toward reducing P450s or other endogenous physiological partners. In contrast, N-terminal-truncated *Saccharomyces*

*Correspondence: larissa.m.podust@vanderbilt.edu
[4]These authors contributed equally to this work.

cerevisiae CPR (yCPR) used for determination of the crystal structure in the present paper can complement *S. cerevisiae* cells with a disrupted CPR gene to reconstitute ergosterol biosynthesis (Venkateswarlu et al., 1998). Purified yCPR supports cytochrome c reduction (Lamb et al., 2001) as well as CYP51 sterol 14α-demethylase and CYP61 sterol 22-desaturase activities (Lamb et al., 1999, 2001; Venkateswarlu et al., 1998). In a search for structural determinants allowing physiological electron transfer between CPR and P450, we determined the crystal structure of yCPR at 2.9 Å resolution. The structure suggests a mechanism of electron transfer in CPR whereby a single FMN molecule shuttles between two protein sites and two flavin electronic states and releases electrons to the acceptor from the second, newly discovered site. The mechanism may be conserved throughout evolution for eukaryotic diflavin reductases.

Results and Discussion

Functional Activity of yCPR

In reconstituted assays, the truncated yCPR used to obtain crystals supported the catalytic activity of human CYP51 and rabbit CYP1A2 (Figures 1A–1C), although less efficiently than full-length rat CPR. Thus, lanosterol demethylation by human CYP51 driven by yCPR was almost ten times slower than that by full-length rat CPR (Figure 1A), and it was comparable with the turnover rates for endogenous yeast partners, CYP51 and CYP61, obtained elsewhere (Lamb et al., 1999; Venkateswarlu et al., 1998). In the CYP1A2 catalytic assay, concentrations of yCPR an order of magnitude higher compared to the full-length rat reductase were used to obtain equal amounts of O-demethylated 7-methoxyresorufin (Figure 1B). However, even this reduced functional activity of yCPR is in direct contrast to the truncated form of rat CPR, which is unable to support any P450 activities (Wang et al., 1997). This difference is somewhat surprising because overall rms deviations for backbone atoms between yCPR and rCPR in the crystal structures are within 1.44 Å, which indicates a high similarity between these two proteins.

The Connecting Domain in yCPR Binds FMN and FAD Cofactors

The most striking feature of the yCPR compared to the rCPR is the presence of a second FMN cofactor (FMN2) bound to the interface of the connecting and the FMN binding domains (Figure 2A), so that the dimethylbenzene edge of the FMN2 isoalloxazine, specifically the 8-CH_3 group, protrudes from below the protein surface toward two nearby acidic clusters, ^{186}D-D^{187} and ^{193}D-E-D^{195} (^{207}D-D-D^{209} and ^{213}E-E-D^{215} in the rCPR), a surface to which cytochrome c and P450 are mapped to bind (Nisimoto, 1986; Nisimoto and Otsuka-Murakami, 1988; Shen and Kasper, 1995) (Figure 2B). Another notable feature that distinguishes the yeast and rat CPR structures is the conformation of the FAD adenosine moiety, which in yCPR is bound between residues P365 and Y405 in a hydrophobic pocket in the connecting domain (Figure 2C). However, in rCPR, it is exposed to the large opening within the protein interior, where it can potentially clash with the phosphate group of FMN2. Hence, in yCPR, the plane of the isoalloxazine ring of FMN2 is orientated at ~60° from the FAD adenosine moiety and is separated from it by a residue of the connecting domain P365 (*si* face of FMN2). The Y75 of the FMN binding domain is on the *re* face of FMN2. In rCPR, spatial hindrance created by the bulk of the FAD adenosine may prevent FMN from binding in the FMN2

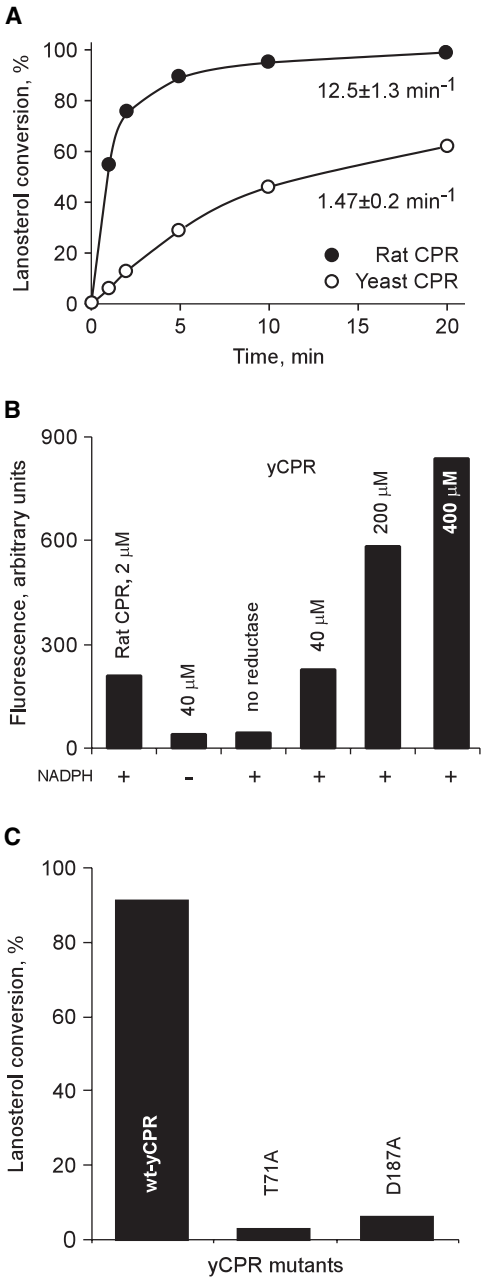

Figure 1. Functional Activity Assays

(A) Time course of lanosterol 14α-demethylation by human CYP51 driven by full-length rat and truncated yeast CPR. CYP51 is at a concentration of 2 μM, and both reductases are at a concentration of 4 μM. Turnover numbers are indicated below each curve and are given in nmol product formed/min/nmol CYP51.

(B) O-demethylation of 7-methoxyresorufin by rabbit CYP1A2. Concentrations of CYP1A2 were 20 μM for yCPR and 2 μM for full-length rat CPR-driven reactions.

(C) Functional activity of the yCPR mutants in lanosterol 14α-demethylation by human CYP51.

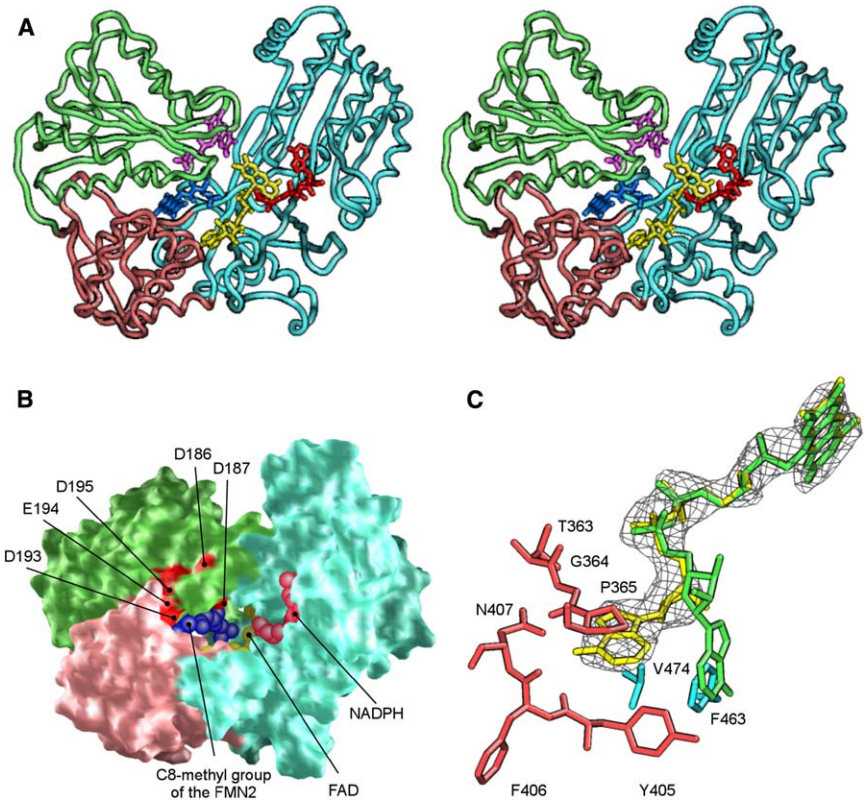

Figure 2. Overall yCPR Structure

(A) Stereoview of the overall yCPR structure with four cofactors bound: FMN1, purple; FMN2, blue; FAD, yellow; NADPH, magenta. FMN2 is closer to the viewer and is located between the FMN binding domain (green) and the connecting domain (rose). 7- and 8-CH_3 groups of the FMN2 point toward the viewer. 7- and 8-methyl groups of FMN1 point toward the same groups of the FAD. The FAD/NADPH binding domain is shown in cyan.

(B) A surface view of the structure in the same color scheme and same orientation as in (A). Negatively charged clusters of residues involved in cytochrome c and P450 binding are in red. The FMN2 (blue) is clearly visible through the bowl opening. Its 8-CH_3 group points though the opening toward the bulk solvent.

(C) Superimposition of FAD in the yCPR (yellow) and FAD in the rCPR (green). The electron density for FAD in the yCPR is represented by a fragment of the $2F_o - F_c$ composite omit map contoured at 1.8σ. The FAD adenosine moiety in the yCPR is bound in a hydrophobic pocket formed by residues of the connecting (rose) and the FAD/NADPH binding (cyan) domains.

site despite the fact that the isoalloxazine binding portion of the FMN2 site is well-defined, and excess FMN was used to obtain the rCPR crystals (Wang et al., 1997).

The FMN1 Site

The FMN1 site is located in the CPR flavodoxin domain and is buried within the CPR interior. The FMN1 site is well conserved among all CPRs (Figure 3). The FMN1 isoalloxazine ring in yCPR is bound between aromatic residues Y118 (*re* face) and Y157 (*si* face), while F160 and F159 are at the pyrimidine edge (Figure 4A). Additional contacts between the isoalloxazine ring and the apoprotein are with backbone residues ^{116}S-G^{119} and ^{153}G-N^{161}. The hydroxyl groups of the ribityl moiety are 4 Å away from the invariant D187. The FMN1 phosphate is hydrogen bonded to the hydroxy amino acid S67, S116, and Y118 side chains, and to the backbone amide groups of the conserved quintet of residues Q^{68}T^{69}G^{70}T^{71}A/G^{72}. As in flavodoxins, the negative charge on the phosphate is not neutralized by positively charged amino acids. As a result of this neutral and hydrophobic environment, flavin semiquinone is highly stabilized in flavodoxins at its neutral form (Mayhew and Tollin, 1992), an exception being the isolated P450BM3 flavodoxin domain, which was reported to stabilize an anionic (red) FMN semiquinone (Hanley et al., 2004). Given that the protein backbone is primarily involved in the interactions with the FMN1 isoalloxazine ring, the electronic structure and, consequently, the redox properties of the FMN bound in this site are expected to be similar between CPRs. High sequence similarity in FMN1 binding regions conflicts with the direct and indirect estimations of the reduction potentials of diverse CPRs, demonstrating that the reduction potentials of both FAD and FMN can vary significantly from source to source so that the equilibrium constant of some individual steps of different reductases can differ by orders of magnitude (Murataliev et al., 2004).

The FMN2 Site

The FMN2 site lies at the interface of the flavodoxin and connecting domains. It is exposed to the bulk solvent and is far less conserved across the CPR gene family than the FMN1 site (Figure 3). In fact, only the residues

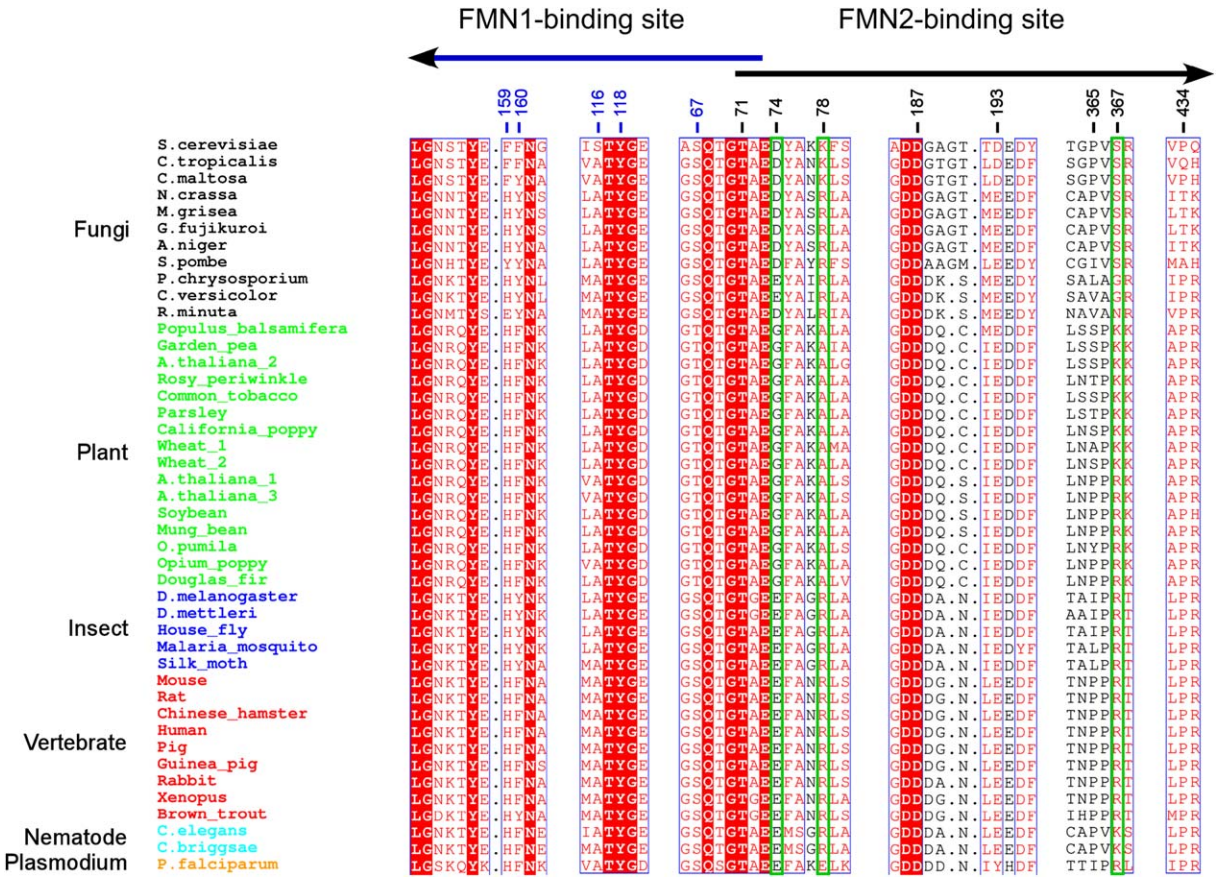

Figure 3. Sequence Alignment for the FMN Binding Sites in the CPR Gene Family

Residues constituting the FMN1 site are labeled with blue numbers, and residues constituting the FMN2 site are labeled with black numbers. The arrows show the direction from the N terminus to the C terminus. Residues interacting with the pyrimidine edge of the FMN2 are enclosed in green boxes. Alignment was performed for 44 CPR sequences by using BCM Search Launcher (Smith et al., 1996; http://searchlauncher.bcm.tmc.edu/multi-align/multi-align.html). The figure was generated with ESPript (Gouet et al., 1999).

binding the FMN2 ribityl moiety, T71 and D187, are invariant in all CPRs. Binding to the isoalloxazine ring shows phyla-specific variations, which potentially may tune the isoalloxazine ring system to its change in redox potential and reactivity in different CPRs. At the hydrophilic pyrimidine edge of the FMN2, charged side chains of residues D74 and K78 are within hydrogen bond distance of the flavin N3 (2.5 Å) and O4 atoms (3.2 Å), respectively (Figures 4B and 5). Negative and positive charges at residues 74 and 78, respectively, are remarkably conserved throughout all CPR species except plant forms, where these positions are occupied by glycine and alanine, respectively (Figure 3).

On the *re* face of the FMN2 isoalloxazine ring, the electronegative Y75 hydroxyl oxygen is centered 3.3 Å above the plane of the central ring (Figures 4B and 5). Y75 is conserved in fungi, but it is substituted by phenylalanine in plants and vertebrates and by methionine in nematodes (Figure 3). On the *si* face, the electron-rich carbonyl oxygen of P365 points at N5 in FMN2 (3.15 Å), defining an angle with the isoalloxazine plane of 110°. The FMN2 ribityl moiety is hydrogen bonded to the carboxyl group of D187 (2.8 Å and 2.5 Å), and this, in turn, is hydrogen bonded to T71 (3.5 Å) (Figures 4B and 5). There are no direct contacts between the FMN2 phosphate group and the protein in the crystal structure. The electron density for FMN2 is progressively less defined toward the phosphate end (Figure 4B). There appears to be enough space in the FMN2 site to accommodate either FMN or FAD. Therefore, to exclude FAD as a third flavin cofactor, crystallization of yCPR was also performed with the addition of only FAD. This resulted in crystals containing an empty FMN2 site, yet the FMN1 site was fully occupied. This fact indicates that the third flavin cofactor bound within yCPR in the crystal is indeed an FMN; the less tight binding of FMN2 is likely due to high accessibility of the FMN2 site at the protein surface.

Flavin Binding in yCPR and Other Flavoproteins

Protein-cofactor interactions observed in the FMN2 site are not random; they are also found in other flavoproteins of diverse functions. Specifically, a positive charge at the pyrimidine edge of the isoalloxazine ring is functionally relevant because it can stabilize an anionic form of the reduced flavin and increase the redox potential of the cofactor (Ghisla and Massey, 1989). The flavoproteins in Table 1 stabilize anionic semiquinone intermediates of the flavin through contact (<3.5 Å distance) with a positive charge—either fully charged side chains of lysine or arginine, or the partially charged N terminus of the α helix or a cluster of peptide nitrogens. Thus, a positive charge at K78 may compensate for the

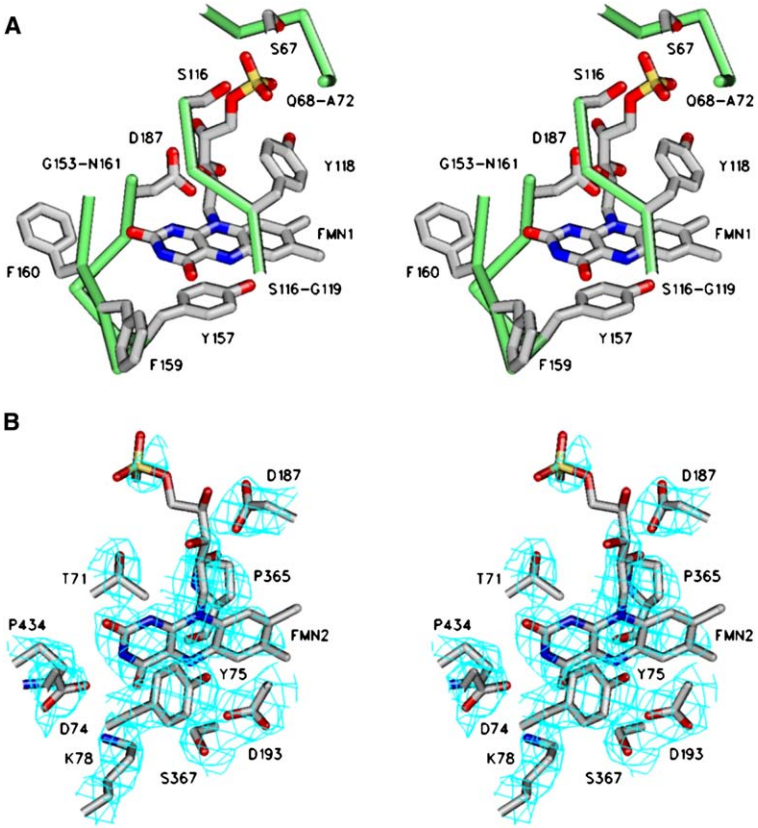

Figure 4. FMN Binding Sites in yCPR

(A and B) Stereoviews of the (A) FMN1 and (B) FMN2 sites. Shown are residues that are within 4 Å of FMNs. The electron density is from the $2F_o - F_c$ composite omit map contoured at 1.3σ. Stretches of the protein backbone in the FMN1 site are shown in green.

negative charge at the C4-O4 locus of the putative anionic semiquinone in the FMN2 site. The flavin N3 atom is commonly found to be hydrogen bonded to proteins, mostly via backbone carbonyl groups and more rarely via amino acid side chains (Becker and Thomas, 2001; Bradley and Swenson, 2001; Fox and Karplus, 1994; Komori et al., 2001; Xia and Mathews, 1990). In yCPR, N3 is hydrogen bonded to D74. In addition, π-π stacking interactions of the electron-rich backbone carbonyl oxygen (P365) with the flavin N5 atom and of the electronegative tyrosine (Y75) with a highly electropositive central ring of the isoalloxazine are observed in many flavoproteins. Thus, the presence of a second FMN cofactor in the yCPR crystals may reveal occupancy of a functional site. Nevertheless, discovery of a second FMN binding site in an electron transporter like CPR that has been studied extensively is surprising and leaves room for concern that this is a possible artifact of crystallization. Questions that arise beyond this concern are: is the FMN2 site functionally important? How many FMN molecules function in the yCPR? Do other CPRs, including the previously crystallized rCPR, have a second FMN binding site? To begin to look for answers, we have performed additional experiments and have further analyzed the yCPR structure and sequence similarity in the CPR gene family.

All CPRs studied to date have an equimolar FAD:FMN ratio. Analysis of the cofactor content in yCPR also reveals an equimolar protein:FMN:FAD ratio, indicating occupancy of apparently only the FMN1 site. The purified protein is functionally active without added FMN, which leads to the conclusion that one FMN molecule is sufficient for yCPR to transfer electrons to P450s. Reduction of excess cytochrome c with the yCPR/NADPH, both in equimolar ratio, generates two reduced cytochrome c molecules per one consumed NADPH, indicating that no priming with NADPH is required and that one- and two-electron-reduced states of yCPR donate electrons to the acceptor. For the FMN2 site to be functionally active, a single FMN has to shuttle between both FMN sites. Thus, occupancy of both FMN sites at the same time must be due to the high concentrations of externally added FMN and the ammonium sulfate in crystallization conditions. From the analysis of the yCPR structure with added FMN, all three flavin cofactors are bound within the empty spacious protein interior that is largely protected from the bulk solvent (Figures 2A and 2B). The relative orientation of both FMN molecules indicates roughly 2-fold rotation symmetry with an axis going through the invariant D187 (Figure 5). For relocation from the FMN1 to the FMN2 site to occur, FMN would have to swing along the interface between the FMN and FAD/NADPH binding domains within the protein interior, thus circumscribing about half of a circle with a 10 Å radius around the invariant D187 as a center of rotation. At the same time, the FMN isoalloxazine ring should rotate about 45° in one direction, and the phosphate group should rotate about 90° in another direction around the ribityl side chain. During this relocation, the ribityl moiety of FMN would remain within the interaction distances from the carboxyl of D187, which is held in position by hydrogen bonding with the T71. As a result of this transition between the FMN1 and the FMN2 sites, the FMN N5-reference atom would relocate ~20 Å, and the 8-CH_3 group would relocate ~16 Å (Figure 5). There is enough space within the protein interior to

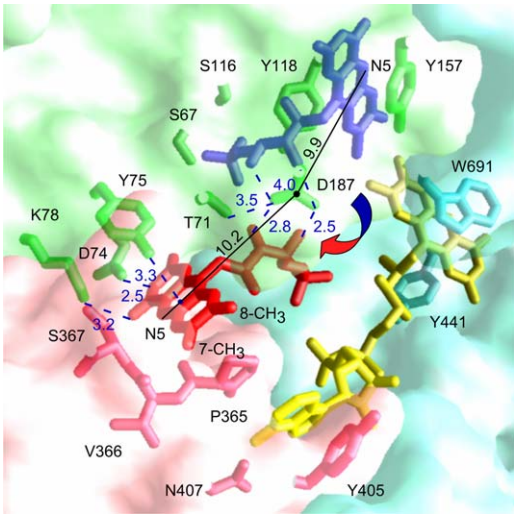

Figure 5. Relative Orientation of FMN1 and FMN2 in yCPR

The orientation of FMN1 (blue) and FMN2 (red) in the structure shows roughly 2-fold rotation symmetry with an axis going through D187. The numbers of angstroms in blue indicate the distances between interacting atoms. The numbers of angstroms in black indicate the distances between the N5-reference atom in FMN and a putative center of rotation, D187. FAD is yellow; the yCPR domains are opaque and are highlighted according to the color scheme in Figure 1. The only clearly visible portion of the FMN2 is the 8-CH_3 group that points toward the bulk solvent.

accommodate this relocation without dissociation of FMN from the reductase. Mutation of D187 and T71 to alanine in yCPR results in almost complete loss of functional activity toward CYP51 (Figure 1C), although activity toward cytochrome c remains unchanged. The concept of flavin motion as an integral part of the catalytic function has been developed for *p*-hydroxybenzoate hydroxylase from *Preudomonas aeruginosa* and *Pseudomonas fluorescens* and related flavoprotein monooxygenases that catalyze hydroxylation of the aromatic ring of a substrate (Entsch et al., 2005). Movement of the flavin between *out* and *in* conformations (7–8 Å) in this enzyme occurs by rotation of the isoalloxazine ring about the ribityl side chain in the plane of the ring and is necessary for reduction by NADPH (*out* conformation) followed by reaction with oxygen (*in* conformation) to form a flavin-C4a-hydroperoxide, an active form of oxygen in flavoprotein hydroxylases.

Hypothetical Structure-Based Mechanism of Electron Transfer in yCPR

The function of CPR is to split two reducing equivalents obtained from NADPH and deliver them to P450 and other acceptor proteins in two one-electron transfer steps. NADPH reduces FAD that, in turn, transfers electrons to FMN. The latter serves as a mediator that delivers electrons to P450. Access to the CPR surface for FMN seems to be necessary to permit delivery of electrons to target proteins. The presence of the two FMN binding sites in yCPR with different environments and accessibilities, and the requirement of only one FMN molecule for electron transfer to P450, leads to a hypothesis that yCPR performs its function through a mechanism similar to *p*-hydroxybenzoate hydroxylase, shuttling a single FMN cofactor between two FMN binding sites. Exposure of the 8-CH_3 group of FMN2 to the bulk solvent between negatively charged clusters of residues involved in protein-acceptor binding suggests that the FMN2 site is a port of exit of yCPR electrons.

We hypothesize that CPR cycles in a 0-2-1-0 sequence, where the numbers indicate the number of electrons residing on the flavins (Figure 6). NADPH binds to oxidized reductase (a), and hydride-ion transfer occurs with transient formation of a charge-transfer complex (b). As a result of intracomplex electron transfer, FMN bound in the first site obtains one electron from FADH and, upon $FMN^{-\bullet}$ protonation, both become neutral (blue) semiquinones, $FADH^{\bullet}$ and $FMNH^{\bullet}$ (c). The neutral $FMNH^{\bullet}$ semiquinone swings along the interface between the FMN and FAD/NADPH binding domains to the FMN2 site as described above (Figure 5). In the second

Table 1. Binding Features of the Pyrimidine Edge of the Isoalloxazine Ring in Flavoproteins of Diverse Functions

Flavoenzyme	Cofactor	PDB ID Code	C2-O2 Contacts	C2-O4 Contacts	References
Old yellow enzyme	FMN	1OYB	R243		(Fox and Karplus, 1994; Nakamura et al., 1965)
Flavocytochrome b2	FMN	1FCB	K349		(Xia and Mathews, 1990)
Trimethylamine dehydrogenase	FMN	2TMD	R222		(Anderson et al., 2000)
Glycolate oxidase	FMN	1GOX	K230		(Massey, 1995)
D-amino acid oxidase	FAD	1DDO	α helix		(Massey, 1995)
Cholesterol oxidase (type I)	FAD	1COY	α helix		(Martinez et al., 1997; Sampson and Vrielink, 2003)
Cholesterol oxidase (type II)	FAD	1I19		R477	(Martinez et al., 1997; Sampson and Vrielink, 2003)
Monoamine oxidase	FAD	1OJA	N-S59, N-Y60		(Yue et al., 1993)
Medium-chain-acylCoA dehydrogenase	FAD	3MDE	N-V135, N-T136		(Mizzer and Thorpe, 1981)
Electron transfer flavoprotein	FAD	1EFV	N-R249, H286	N-Q265, N-T266, N-G267	(Byron et al., 1989; Davidson et al., 1986; Dwyer et al., 1999)
Cytochrome b5 reductase	FAD	1UMK		N-K110	(Iyanagi et al., 1984; Kobayashi et al., 1988)
DNA photolyase	FAD	1IQR	R248		(Schleicher et al., 2005)
Proline dehydrogenase	FAD	1K87		R431	(Becker and Thomas, 2001)

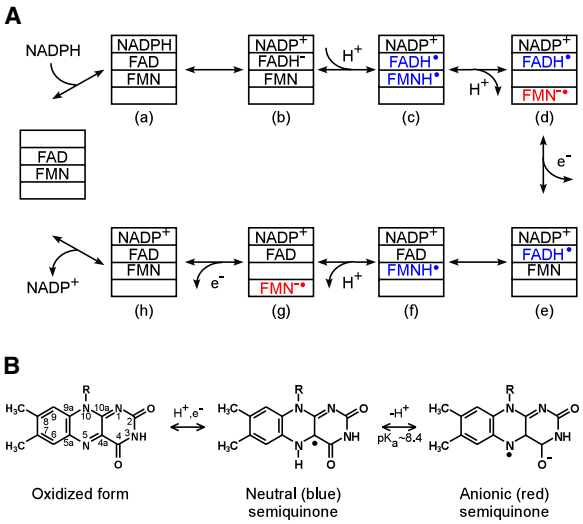

Figure 6. Hypothetical Mechanism of Electron Transfer by P450 Reductases

(A) Single catalytic turnover of yCPR. Neutral semiquinone is shown in blue, and putative anionic semiquinone is shown in red.

(B) Structures of oxidized and semiquinone states of the isoalloxazine system shown with the *si* side facing the viewer.

site, upon deprotonation, the neutral FMNH• semiquinone presumably becomes an anionic FMN-• semiquinone, and the negative charge on C4-O4 is stabilized via the invariant positive charge at position 78 (d); it is in this form that the FMN-• semiquinone donates the first electron to an acceptor. While FMN-• delivers the first electron, the second electron is stored in the form of a neutral FADH• semiquinone. To obtain the second electron, oxidized FMN must swing back to the FMN1 site (e); obtain the second electron from the neutral FADH• semiquinone to become a neutral FMNH• semiquinone, leaving FAD in an oxidized form (f); and repeat translocation to the FMN2–site, becoming, once again, an anionic FMN-• semiquinone (g). Here, FMN-• donates the second electron to the acceptor and returns back to the FMN1 site to regenerate a fully oxidized flavoprotein (h). Finally, $NADP^+$ dissociates from the complex (in principal, $NADP^+$ could leave at any stage from [c] onward).

We speculate that the proposed translocation of FMN may be driven by a flow of the electrons, which must be strictly coupled with protonation-deprotonation of the FMN isoalloxazine ring and relocation of the FMN from one FMN binding site to another. Each time FMN receives or donates an electron, it must relocate to an alternative FMN binding site due to the different amino acid environments of each site, which may be designed to accommodate different electronic forms of the FMN. In vitro, once an electron is released from the semiquinone in the FMN2 site, oxidized FMN may occasionally dissociate from CPR due to more pronounced exposure of the FMN2 site to the bulk solvent and its presumably reduced affinity for the neutral FMN species. Thus, the proposed mechanism explains the well-documented phenomenon that FMN, in contrast to FAD, can be reversibly released from CPR, while, to release FAD, CPR has to be partially denatured (Nisimoto and Shibata, 1982; Vermilion and Coon, 1978). Two questions

Table 2. Crystallographic Data and Statistics

Data Set	Se-Met^{+FMN}	Native^{-FMN}
PDB ID	2BF4	2BN4
Data Collection		
Wavelength, Å	0.97940	0.97918
Resolution, Å	3.0	2.9
Unique reflections	65,903	33,851
Redundancy[a]	7.6 (4.7)	5.4 (4.7)
Coverage, %	99.9 (92.8)	94.4 (75.8)
Space group	$P2_12_12_1$	$P2_12_12_1$
Unit cell (a, b, c), Å	77.75, 87.09, 259.59	78.14, 77.84, 261.49
R_{sym}[b], %	5.8 (30.1)	11.0 (50.6)
I/σ	28.0 (4.3)	16.9 (2.0)
SAD Phasing Statistics		
Number of used sites	18	
Phasing power[c]	1.69	
Figure of merit after phasing	0.31	
Quality of Model		
Protein atoms	10,148	10,028
Heterogen atoms	325	248
Solvent atoms	151	55
Mean B factor, Å^2	53.1	66.7
R_{cryst} (R_{free})[d], %	19.7/26.1	23.3/30.0
Rms deviation		
Bonds, Å	0.008	0.008
Angles, °	1.4	1.5

[a] Numbers in parentheses correspond to the highest-resolution shell.

[b] $R_{sym} = \Sigma|I_i - \langle I\rangle|/\Sigma I_i$, where I_i is the intensity of the i^{th} observation, and $\langle I\rangle$ is the mean intensity of reflection.

[c] Phasing power = $\langle F_h\rangle/E$, in which $\langle F_h\rangle$ is the root mean square heavy atom structure factor, and E is the residual lack of closure.

[d] $R_{cryst} = \Sigma\ ||F_o| - |F_c||/\Sigma|F_o|$, calculated with the working reflection set. R_{free} is the same as R_{cryst}, but it is calculated with the reserved reflection set.

arise: How high is the energy barrier for FMN translocation? To what degree do structural fluctuations in CPR facilitate the FMN shuttling? The observation that a single hydrogen bond formed between the flavin and the hydroxyl group of the substrate analog shifts the isoalloxazine to the *out* position in *p*-hydroxybenzoate hydroxylase highlights the small energy barriers for such changes in that enzyme (Entsch et al., 2005). In yCPR, the ribityl side chain of the FMN apparently preserves contacts with D187 upon translocation to the FMN2 site. The isoalloxazine ring could relocate in a different environment with multiple interactions with the protein side chains, which are not necessarily weaker than those in the FMN1 site considering the fact that FMN may have different electronic states in each site. FMN phosphate is hydrogen bonded to the hydroxyl of the side chains and the amide nitrogen of the backbone in the FMN1 site, and no electrostatic interactions compensate for the negative charge of the phosphate group. Contacts between the FMN2 phosphate group and yCPR are missing in the current structure. We anticipate that in the case of physiological occupancy of the FMN2 site, which we believe suggests an empty FMN1 site, some conformational changes may occur to facilitate the formation of such contacts and to lower the energy barrier for the FMN translocation.

Mechanisms of Electron Transfer in P450 Reductases

The nature of the active form of FMN is one of the main controversies between mechanisms of electron transfer in mammalian versus other P450 monooxygenase systems. Data obtained on the reductases competent in physiological electron transfer to P450s, including house fly CPR (Murataliev et al., 1999; Murataliev and Feyereisen, 1999) and P450BM3 reductase (Murataliev et al., 1997; Sevrioukova et al., 1996a), indicate a 0-2-1-0 cycling sequence for the reductase reduction state, no need for a priming reaction, donation of electrons from the FMN semiquinone, and formation of two types of FMN semiquinone. All of these features are present in the structure-based mechanism proposed herein. In contrast, two different mechanisms are proposed for mammalian reductases with the enzyme reduction state cycling through 1-3-2-1 or 2-4-3-2 sequences (Backes, 1993). Both mechanisms require a priming reaction with NADPH to bring the reduction state of the flavoprotein to either 3 or 4 before any electron transfer from FMN to an acceptor can occur, implying that the FMN hydroquinone, but not its semiquinone, serves as a donor of both electrons. All one-electron-reduced CPRs can stabilize an air-stable, neutral semiquinone that does not efficiently reduce P450 or cytochrone c (Backes, 1993; Murataliev et al., 2004). Analysis of available data on microsomal CPRs presented in Murataliev et al. (2004) indicates a number of observations that disagree with either of the mechanisms proposed for mammalian CPR and suggests that a catalytic role for an FMN semiquinone in mammalian CPRs may have been largely overlooked. The absence of FMN in the FMN2 site in the rCPR may be directly related to the inability of N-terminal-truncated mammalian CPRs to perform physiologically relevant electron transfer (Backes, 1993; Hayashi et al., 2003). Apparently, N-terminal truncation of yCPR does not have such a severe impact on its functional activity, although the exact reason for this is unknown.

The yCPR structure has revealed a second FMN binding site in the interface of the connecting and the FMN binding domains. The two FMN binding sites have different accessibilities and amino acid environments, the latter suggesting stabilization of different electronic forms of flavin semiquinone: neural (blue) in FMN1 sites and anionic (red) in FMN2 sites. Considering the fact that only one FMN molecule is required for function, a hypothetical structure-based mechanism is proposed that includes FMN shuttling between the two sites as a novel, to our knowledge, feature. Given the complexity of electron transfer in CPR, a full understanding of the functional role of this newly, to our knowledge, discovered site and applicability of the proposed mechanism will require further crystallographic analysis and thermodynamic measurements on the CPR with specifically designed mutants, as well as kinetic measurements directed at elucidating the order of events. The results presented here provide testable hypotheses for new experiments to address each aspect of the mechanism of intramolecular electron transfer in yCPR. UV-Vis, stopped-flow, fluorescence, and EPR spectrophotometric approaches will be used to attempt assignment of distinct spectroscopic signatures to the various binding and redox configurations of FMN and FAD. Anaerobic stopped-flow studies with an OLIS RSM-1000 instrument will give a set of complete UV-Vis spectra as a function of time, which in addition to analysis by singular value decomposition should be specific to the number of absorbing species if not their identities. EPR spectroscopy, which will be used to detect FMN semiquinone radicals, can distinguish between the neutral and anionic forms of FMN semiquinone and may be able to distinguish different binding environments. Mutants with targeted ability to shuttle FMN or with changed environment in the FMN2 site are generated as comparative companions of the wild-type yCPR for these studies. Another direction that we will pursue is screening for the potential CPR inhibitors that bind in the FMN2 site. To rapidly screen a large number of compounds, we adapted a fluorescence assay (Prough et al., 1978) utilizing the ability of CYP1A2 to convert 7-methoxyresorufin to fluorescent resorufin. The yCPR inhibitors identified as a result of screening will be used in functional assays to refine our understanding of another aspect of the mechanism: intermolecular electron transfer between CPR and protein acceptors. We believe that the discovery of the second FMN binding site will change the current understanding of CPR structure-function and lead to resolution of mechanistic controversies between different CPR families. The understanding of these processes will have more widespread implications because other diflavin reductases, e.g., nitric oxide synthase and methionine synthase reductase, are highly homologous genetically, structurally, and functionally.

Experimental Procedures

Activity of Truncated yCPR in Reconstituted Assays

The truncated form of yCPR lacking 33 residues, including the N-terminal hydrophobic membrane anchor, and containing 6 N-terminal histidine residues preceded by 4 and followed by 15 residues from the cloning site (Venkateswarlu et al., 1998) was expressed in *E. coli* and was purified to homogeneity by affinity chromatography on Ni-NTA agarose (Qiagen), followed by ion-exchange chromatography on S-Sepharose and Q-Sepharose (both from Amersham Pharmacia Biotech).

Functional activity assays were performed with human sterol 14α-demethylase (CYP51), rabbit CYP1A2 with 7-methoxyresorufin as a substrate, and cytochrome c. The reaction of lanosterol 14α-demethylation was carried out at a 1:2 P450:CPR molar ratio. Samples contained 2 μM CYP51, 50 μM lanosterol (cold/[3-^{3}H] [American Radiolabeled Chemicals, Inc.] mixture, 10^5 cpm), 100 μM dilauroyl-α phosphatidylcholine, 0.4 mg/ml isocitrate dehydrogenase, 25 mM sodium isocitrate, and 5 mM NADPH in 0.5 ml of 20 mM MOPS (pH 7.4), 50 mM KCl, 5 mM $MgCl_2$, 10% (v/v) glycerol. The reaction was terminated after 20 min of incubation at 37ºC by the addition of ethyl acetate, and sterols were subsequently extracted. The enzyme-derived products were analyzed by reverse-phase (C18) HPLC (Waters Corporation, USA) equipped with a β-RAM Detector (Inus Systems, Inc., USA) by using a linear gradient of acetonitrile: water:methanol (4.5:1:4.5)/methanol as a mobile phase at the flow rate of 1.5 ml/min.

The enzymatic reaction of O-demethylation of 7-methoxyresorufin by CYP1A2 was carried out at a variety of yCPR concentrations as indicated in Figure 1B. Samples contained 20 μM CYP1A2, 50 μM 7-methoxyresorufin, 100 μM dilauroyl-α phosphatidylcholine, and 5 mM NADPH in 100 μl of 20 mM K-phosphate (pH 7.5). The reaction was terminated after 20 min of incubation at 37ºC by the addition of 100 μl methanol. Product formation was monitored by a fluorometric assay (Prough et al., 1978) (excitation 544 nm, emission 590 nm) by using a FLUOstar automated microplate reader (BMG Lab Technologies GmbH, Germany). Rabbit CYP1A2 and 7-methoxyresorufin were kind gifts of F.P. Guengerich.

Reduction of cytochrome c with yCPR, wild-type, and T71A and D187A mutants was carried out in 1 ml of 100 mM K-phosphate buffer (pH 7.7) containing 10 μM reductase and 40 μM cytochrome c. Reactions were initiated by adding NADPH to 10 μM concentration. Accumulation of reduced cytochrome c was monitored by visible light spectroscopy at 550 nm by using $\varepsilon = 21{,}000\ M^{-1}cm^{-1}$. Two molecules of cytochrome c were reduced per one NADPH molecule consumed during a reaction driven by the wild-type and both mutants.

Stoichiometry of Flavin Cofactors

yCPR was denatured by heating at 95ºC for 30 min, the precipitate was removed by centrifugation, and the supernatant was analyzed isocratically by reverse-phase HPLC (Waters Corporation, USA) equipped with a 996 Photodiode Detector by using 10 mM diammonium hydrogen phosphate (pH 5.5):acetonitrile (10:1.2) (Pietta et al., 1982) as a mobile phase at the flow rate of 1.0 ml/min. The content and ratio of cofactors were determined with calibration curves from the HPLC profiles at 473 nm by using $\varepsilon = 9200\ M^{-1}cm^{-1}$ for both FMN and FAD (Aliverti et al., 1999). Protein concentration was measured with the BCA Protein Assay Reagent (Pierce). The ratios of protein/FMN/FAD obtained from two experiments are 1.0:0.9:1.0 and 1.0:1.1:1.2.

Crystallization and Data Collection

Crystals of yCPR were obtained in the presence of externally added cofactors, FMN, FAD, and NADPH, at 1 mM concentrations. Alternatively, FMN was omitted, while FAD and NADPH were added. Two crystal forms belonging to the orthorhombic $P2_12_12_1$ space group with different unit cell parameters (Table 2) grew from 0.2 mM yCPR, in a selenomethionine-derived or native form, in 10 mM Tris-HCl (pH 7.5), 100 mM NaCl in a hanging drop equilibrated against 1.6 M ammonium sulfate in 100 mM sodium citrate buffer (pH 5.0). Native and single anomalous dispersion diffraction data (Table 2) were collected at 100–110 K at the Southeast Regional Collaborative Access Team (SER-CAT) 22ID and Structural Biology Center 19ID beamlines, Advanced Photon Source, Argonne National Laboratory, USA.

Phasing and Refinement

The images were integrated, and the intensities were merged by using HKL2000 (Otwinowski and Minor, 1997). The positions of selenomethionine sites were determined for the first crystal form by using the SAD protocol in CNS (Brunger et al., 1998). The phases were calculated and improved by CNS, yielding an interpretable electron density map at 3.0 Å resolution. The structure of the second crystal form with no added FMN was determined by molecular replacement to a resolution of 2.9 Å. The final atomic models (Table 2) were obtained after 15 and 6 iterations of refinement (CNS [Brunger et al., 1998]) and manual model building with the program O (Jones et al., 1991), respectively.

Acknowledgments

We thank Dr. Andrew Munro, University of Leicester, UK, and Dr. Jorge Capdevila, Vanderbilt University, for discussions and helpful suggestions and the Southeast Regional Collaborative Access Team (SER-CAT) Argonne National Laboratory for assistance with data collection. The Vanderbilt Molecular Recognition Unit was funded in part by National Institutes of Health (NIH) CA68485. This work was supported by the Vanderbilt University Medical Center Discovery Grant Program (to L.M.P.), NIH grants GM37942, GM067871, and ES00267 (to M.R.W.), a Wellcome Trust grant (to D.C.L.), and a Biotechnology and Biological Sciences Research Council grant (to D.C.L and S.L.K).

Received: August 5, 2005
Revised: September 19, 2005
Accepted: September 19, 2005
Published: January 10, 2006

References

Aliverti, A., Curti, B., and Vanoni, M.A. (1999). Identifying and quantitating FAD and FMN in simple and in iron-sulfur-containing flavoproteins. In Methods in Molecular Biology. Flavoprotein Protocols, S.K. Chapman, and G.A. Reid, eds. (Totowa, NJ: Humana Press, Inc.), pp. 9–24.

Anderson, R.F., Jang, M.H., and Hille, R. (2000). Radiolytic studies of trimethylamine dehydrogenase. Spectral deconvolution of the neutral and anionic flavin semiquinone, and determination of rate constants for electron transfer in the one-electron reduced enzyme. J. Biol. Chem. *275*, 30781–30786.

Backes, W.L. (1993). NADPH-cytochrome P450 reductase: function. In Handbook of Experimental Pharmacology: Cytochrome P450, J.B. Schemkmann, and H. Greim, eds. (Berlin, NY: Springer), pp. 15–34.

Becker, D.F., and Thomas, E.A. (2001). Redox properties of the PutA protein from *Escherichia coli* and the influence of the flavin redox state on PutA-DNA interactions. Biochemistry *40*, 4714–4721.

Bradley, L.H., and Swenson, R.P. (2001). Role of hydrogen bonding interactions to N(3)H of the flavin mononucleotide cofactor in the modulation of the redox potentials of the *Clostridium beijerinckii* flavodoxin. Biochemistry *40*, 8686–8695.

Bredt, D.S., Hwang, P.M., Glatt, C.E., Lowenstein, C., Reed, R.R., and Snyder, S.H. (1991). Cloned and expressed nitric oxide synthase structurally resembles cytochrome P-450 reductase. Nature *351*, 714–718.

Brunger, A.T., Adams, P.D., Clore, G.M., Delano, W.L., Gros, P., Grosse-Kunstleve, R.W., Jiang, J.-S., Kuszewski, J., Nilges, M., and Pannu, N.S. (1998). Crystallography and NMR system: a new software suite for macromolecular structure determination. Acta Crystallogr. D Biol. Crystallogr. *54*, 905–921.

Byron, C.M., Stankovich, M.T., Husain, M., and Davidson, V.L. (1989). Unusual redox properties of electron-transfer flavoprotein from *Methylophilus methylotrophus*. Biochemistry *28*, 8582–8587.

Coves, J., Zeghouf, M., Macherel, D., Guigliarelli, B., Asso, M., and Fontecave, M. (1997). Flavin mononucleotide-binding domain of the flavoprotein component of the sulfite reductase from *Escherichia coli*. Biochemistry *36*, 5921–5928.

Davidson, V.L., Husain, M., and Neher, J.W. (1986). Electron transfer flavoprotein from *Methylophilus methylotrophus*: properties, comparison with other electron transfer flavoproteins, and regulation of expression by carbon source. J. Bacteriol. *166*, 812–817.

Dwyer, T.M., Zhang, L., Muller, M., Marrugo, F., and Frerman, F. (1999). The functions of the flavin contact residues, αArg249 and βTyr16, in human electron transfer flavoprotein. Biochim. Biophys. Acta *1433*, 139–152.

Enoch, H.G., and Strittmatter, P. (1979). Cytochrome b5 reduction by NADPH-cytochrome P-450 reductase. J. Biol. Chem. *254*, 8976–8981.

Entsch, B., Cole, L.J., and Ballou, D.P. (2005). Protein dynamics and electrostatics in the function of p-hydroxybenzoate hydroxylase. Arch. Biochem. Biophys. *433*, 297–311.

Fox, K.M., and Karplus, P.A. (1994). Old yellow enzyme at 2 Å resolution: overall structure, ligand binding, and comparison with related flavoproteins. Structure *2*, 1089–1105.

Ghisla, S., and Massey, V. (1989). Mechanisms of flavoprotein-catalyzed reactions. Eur. J. Biochem. *181*, 1–17.

Gouet, P., Courcelle, E., Stuart, D.I., and Metoz, F. (1999). ESPript: multiple sequence alignments in PostScript. Bioinformatics *15*, 305–308.

Gustafsson, M.C.U., Roitel, O., Marshall, K.R., Noble, M.A., Chapman, S.K., Pessegueiro, A., Fulco, A.J., Cheesman, M.R., Wachenfeldt, C., and Munro, A.W. (2004). Expression, purification, and characterization of *Bacillus subtilis* cytochromes P450 CYP102A2 and CYP102A3: flavocytochrome homologues of P450 BM3 from *Bacillus megaterium*. Biochemistry *43*, 5474–5487.

Hanley, S.C., Ost, T.W., and Daff, S. (2004). The unusual redox properties of flavocytochrome P450 BM3 flavodoxin domain. Biochem. Biophys. Res. Commun. *325*, 1418–1423.

Hayashi, S., Omata, Y., Sakamoto, H., Hara, T., and Noguchi, M. (2003). Purification and characterization of a soluble form of rat liver NADPH-cytochrome P-450 reductase highly expressed in *Escherichia coli*. Protein Expr. Purif. *29*, 1–7.

Ilan, Z., Ilan, R., and Cinti, D.L. (1981). Evidence for a new physiological role of hepatic NADPH:ferricytochrome (P-450) oxidoreductase. Direct electron input to the microsomal fatty acid chain elongation system. J. Biol. Chem. *256*, 10066–10072.

Iyanagi, T., Watanabe, S., and Anan, K.F. (1984). One-electron oxidation-reduction properties of hepatic NADH-cytochrome b5 reductase. Biochemistry *23*, 1418–1425.

Jenkins, C.M., and Waterman, M.R. (1998). NADPH-flavodoxin reductase and flavodoxin from *Escherichia coli*: characteristics as a soluble microsomal P450 reductase. Biochemistry *37*, 6106–6113.

Jones, T.A., Zou, J.Y., Cowan, S.W., and Kjeldgaard, M. (1991). Improved methods for building protein models in electron density maps and the location of errors in these models. Acta Crysallogr. A *47*, 110–119.

Kitazume, T., Takaya, N., Nakayama, N., and Shoun, H. (2000). *Fusarium oxysporum* fatty-acid subterminal hydroxylase (CYP505) is a membrane-bound eukaryotic counterpart of *Bacillus megaterium* cytochrome P450BM3. J. Biol. Chem. *275*, 39734–39740.

Kobayashi, K., Iyanagi, T., Ohara, H., and Hayashi, K. (1988). One-electron reduction of hepatic NADH-cytochrome b5 reductase as studied by pulse radiolysis. J. Biol. Chem. *263*, 7493–7499.

Komori, H., Masui, R., Kuramitsu, S., Yokoyama, S., Shibata, T., Inoue, Y., and Miki, K. (2001). Crystal structure of thermostable DNA photolyase: pyrimidine-dimer recognition mechanism. Proc. Natl. Acad. Sci. USA *98*, 13560–13565.

Laden, B.P., Tang, Y., and Porter, T.D. (2000). Cloning, heterologous expression, and enzymological characterization of human squalene monooxygenase. Arch. Biochem. Biophys. *374*, 381–388.

Lamb, D.C., Kelly, D.E., Venkateswarlu, K., Manning, N.J., Bligh, H.F., Schunck, W.H., and Kelly, S.L. (1999). Generation of a complete, soluble, and catalytically active sterol 14 α-demethylase-reductase complex. Biochemistry *38*, 8733–8738.

Lamb, D.C., Warrilow, A.G.S., Venkateswarlu, K., Kelly, D.E., and Kelly, S.L. (2001). Activities and kinetic mechanisms of native and soluble NADPH-cytochrome P450 reductase. Biochem. Biophys. Res. Commun. *286*, 48–54.

Leclerc, D., Wilson, A., Dumas, R., Gafuik, C., Song, D., Watkins, D., Heng, H.H.Q., Rommens, J.M., Scherer, S.W., Rosenblatt, D.S., and Gravel, R.A. (1998). Cloning and mapping of a cDNA for methionine synthase reductase, a flavoprotein defective in patients with homocystinuria. Proc. Natl. Acad. Sci. USA *95*, 3059–3064.

Martinez, J.I., Alonso, P.J., Gomez-Moreno, C., and Medina, M. (1997). One- and two-dimensional ESEEM spectroscopy of flavoproteins. Biochemistry *36*, 15526–15537.

Massey, V. (1995). Introduction: flavoprotein structure and mechanism. FASEB J. *9*, 473–475.

Mayhew, S.G., and Tollin, G. (1992). General properties of flavodoxins. In Chemistry and Biochemistry of Flavoenzymes, F. Muller, ed. (Boca Raton, FL: CRC Press), pp. 389–426.

Mizzer, J.P., and Thorpe, C. (1981). Stabilization of the red semiquinone form of pig kidney general acyl-CoA dehydrogenase by acyl coenzyme A derivatives. Biochemistry *20*, 4965–4970.

Murataliev, M.B., and Feyereisen, R. (1999). Mechanism of cytochrome P450 reductase from the house fly: evidence for an FMN semiquinone as electron donor. FEBS Lett. *453*, 201–204.

Murataliev, M.B., Klein, M., Fulco, A., and Feyereisen, R. (1997). Functional interactions in cytochrome P450BM3: flavin semiquinone intermediates, role of NADP(H), and mechanism of electron transfer by the flavoprotein domain. Biochemistry *36*, 8401–8412.

Murataliev, M.B., Arino, A., Guzov, V.M., and Feyereisen, R. (1999). Kinetic mechanism of cytochrome P450 reductase from the house fly (*Musca domestica*). Insect Biochem. Mol. Biol. *29*, 233–242.

Murataliev, M.B., Feyereisen, R., and Walker, F.A. (2004). Electron transfer by diflavin reductases. Biochim. Biophys. Acta *1698*, 1–26.

Nakamura, T., Yoshimura, J., and Ogura, Y. (1965). Action mechanism of the old yellow enzyme. J. Biochem. (Tokyo) *57*, 554–564.

Narhi, L.O., and Fulco, A.J. (1986). Characterization of a catalytically self-sufficient 119,000-dalton cytochrome P-450 monooxygenase induced by barbiturates in *Bacillus megaterium*. J. Biol. Chem. *261*, 7160–7169.

Nisimoto, Y. (1986). Localization of cytochrome c-binding domain on NADPH-cytochrome P-450 reductase. J. Biol. Chem. *261*, 14232–14239.

Nisimoto, Y., and Otsuka-Murakami, H. (1988). Cytochrome b5, cytochrome c, and cytochrome P-450 interactions with NADPH-cytochrome P-450 reductase in phospholipid vesicles. Biochemistry *27*, 5869–5876.

Nisimoto, Y., and Shibata, Y. (1982). Studies on FAD- and FMN-binding domains in NADPH-cytochrome P-450 reductase from rabbit liver microsomes. J. Biol. Chem. *257*, 12532–12539.

Ono, T., and Bloch, K. (1975). Solubilization and partial characterization of rat liver squalene epoxidase. J. Biol. Chem. *250*, 1571–1579.

Ostrowski, J., Barber, M.J., Rueger, D.C., Miller, B.E., Siegel, L.M., and Kredich, N.M. (1989). Characterization of the flavoprotein moieties of NADPH-sulfite reductase from *Salmonella typhimurium* and *Escherichia coli*. Physicochemical and catalytic properties, amino acid sequence deduced from DNA sequence of cysJ, and comparison with NADPH-cytochrome P-450 reductase. J. Biol. Chem. *264*, 15796–15808.

Otwinowski, Z., and Minor, W. (1997). Processing of x-ray diffraction data collected in oscillation mode. Methods Enzymol. *276*, 307–326.

Paine, M.J.I., Garner, A.P., Powell, D., Sibbald, J., Sales, M., Pratt, N., Smith, T., Tew, D.G., and Wolf, C.R. (2000). Cloning and characterization of a novel human dual flavin reductase. J. Biol. Chem. *275*, 1471–1478.

Pietta, P., Calatroni, A., and Rava, A. (1982). Hydrolysis of riboflavin nucleotides in plasma monitored by high-performance liquid chromatography. J. Chromatogr. *229*, 445–449.

Porter, T.D., and Kasper, C.B. (1985). Coding nucleotide sequence of rat NADPH-cytochrome P-450 oxidoreductase cDNA and identification of flavin-binding domains. Proc. Natl. Acad. Sci. USA *82*, 973–977.

Porter, T.D., and Kasper, C.B. (1986). NADPH-cytochrome P-450 oxidoreductase: flavin mononucleotide and flavin adenine dinucleotide domains evolved from different flavoproteins. Biochemistry *25*, 1682–1687.

Prough, R.A., Burke, M.D., and Mayer, R.T. (1978). Direct fluorometric methods for measuring mixed-function oxidase activity. Methods Enzymol. *52*, 372–377.

Sampson, N.S., and Vrielink, A. (2003). Cholesterol oxidases: a study of nature's approach to protein design. Acc. Chem. Res. *36*, 713–722.

Schacter, B.A., Nelson, E.B., Marver, H.S., and Masters, B.S.S. (1972). Immunochemical evidence for an association of heme oxygenase with the microsomal electron transport system. J. Biol. Chem. *247*, 3601–3607.

Schleicher, E., Hessling, B., Illarionova, V., Bacher, A., Weber, S., Richter, G., and Gerwert, K. (2005). Light-induced reactions of *Escherichia coli* DNA photolyase monitored by Fourier transform infrared spectroscopy. FEBS J. *272*, 1855–1866.

Sevrioukova, I., Shaffer, C., Ballou, D.P., and Peterson, J.A. (1996a). Equilibrium and transient state spectrophotometric studies of the mechanism of reduction of the flavoprotein domain of P450BM-3. Biochemistry *35*, 7058–7068.

Sevrioukova, I., Truan, G., and Peterson, J.A. (1996b). The flavoprotein domain of P450BM-3: expression, purification, and properties of the flavin adenine dinucleotide- and flavin mononucleotide-binding subdomains. Biochemistry *35*, 7528–7535.

Sevrioukova, I., Truan, G., and Peterson, J.A. (1997). Reconstitution of the fatty acid hydroxylase activity of cytochrome P450BM-3 utilizing its functional domains. Arch. Biochem. Biophys. *340*, 231–238.

Shen, A.L., and Kasper, C.B. (1995). Role of acidic residues in the interaction of NADPH-cytochrome P450 oxidoreductase with cytochrome P450 and cytochrome c. J. Biol. Chem. *270*, 27475–27480.

Smith, G.C., Tew, D.G., and Wolf, C.R. (1994). Dissection of NADPH-cytochrome P450 oxidoreductase into distinct functional domains. Proc. Natl. Acad. Sci. USA *91*, 8710–8714.

Smith, R.F., Wiese, B.A., Wojzynski, M.K., Davison, D.B., and Worley, K.C. (1996). BCM Search Launcher—an integrated interface to molecular biology data base search and analysis services available on the World Wide Web. Genome Res. *6*, 454–462.

Venkateswarlu, K., Lamb, D.C., Kelly, D.E., Manning, N.J., and Kelly, S.L. (1998). The N-terminal membrane domain of yeast NADPH-cytochrome P450 (CYP) oxidoreductase is not required for catalytic activity in sterol biosynthesis or in reconstitution of CYP activity. J. Biol. Chem. *273*, 4492–4496.

Vermilion, J.L., and Coon, M.J. (1978). Identification of the high and low potential flavins of liver microsomal NADPH-cytochrome P-450 reductase. J. Biol. Chem. *253*, 8812–8819.

Wang, M., Roberts, D.L., Paschke, R., Shea, T.M., Masters, B.S., and Kim, J.J. (1997). Three-dimensional structure of NADPH-cytochrome P450 reductase: prototype for FMN- and FAD-containing enzymes. Proc. Natl. Acad. Sci. USA *94*, 8411–8416.

Williams, C.H., Jr., and Kamin, H. (1962). Microsomal triphosphopyridine nucleotide-cytochrome c reductase of liver. J. Biol. Chem. *237*, 587–595.

Xia, Z.X., and Mathews, F.S. (1990). Molecular structure of flavocytochrome b2 at 2.4 A resolution. J. Mol. Biol. *212*, 837–863.

Yue, K.T., Bhattacharyya, A.K., Zhelyaskov, V.R., and Edmondson, D.E. (1993). Resonance Raman spectroscopic evidence for an anionic flavin semiquinone in bovine liver monoamine oxidase. Arch. Biochem. Biophys. *300*, 178–185.

Accession Numbers

The atomic coordinates have been deposited in the Protein Data Bank under ID codes 2BF4 and 2BN4.